

# Mouse apolipoprotein J: characterization of a gene implicated in atherosclerosis

Tuajuanda C. Jordan-Starck,\* S. Diane Lund,<sup>†,\*</sup> David P. Witte,<sup>†</sup> Bruce J. Aronow,<sup>§</sup> Catherine A. Ley,\* William D. Stuart,\* Debi K. Swertfeger,\*\* Lisa R. Clayton,\* Stephen F. Sells,\* Beverly Paigen,<sup>‡</sup> and Judith A. K. Harmony<sup>2,\*.\*.\*</sup>

Departments of Pharmacology and Cell Biophysics,\* Pathology and Laboratory Medicine,<sup>†</sup> Pediatrics,<sup>§</sup> and the Developmental Biology Graduate Program,\*\* College of Medicine, University of Cincinnati, Cincinnati, OH 45267; and Children's Hospital Medical Center, Elland and Bethesda Avenues, Cincinnati, OH 45229; and The Jackson Laboratory,<sup>‡</sup> Bar Harbor, ME 04609

**Abstract** Apolipoprotein J (apoJ), a glycoprotein associated with subclasses of plasma high density lipoproteins (HDL), was found to accumulate in aortic lesions in a human subject with transplantation-associated arteriosclerosis and in mice fed a high-fat atherogenic diet. Foam cells present in mouse aortic valve lesions expressed apoJ mRNA, suggesting local synthesis contributes to apoJ's localization in atherosclerotic plaque. As a prerequisite for elucidating the physiological function of apoJ by using a mouse model, cDNA clones representing the mouse homolog of apoJ were isolated, characterized, and sequenced. The nucleotide sequence predicts a 448 amino acid, 50,260 dalton protein. There was 81% nucleotide sequence similarity between mouse and human apoJ, and 75% similarity at the amino acid level. Mouse apoJ contains six potential N-glycosylation sites, a potential Arg-Ser cleavage site to generate  $\alpha$  and  $\beta$  subunits, a cluster of five cysteine residues in each subunit, three putative amphipathic helices, and four potential heparin-binding domains. Southern blot analysis indicates that the gene encompasses ~23 kb of DNA. Recombinant inbred strains were used to map apoJ to mouse chromosome 14, tightly linked to Mtv-11. All of the transcribed portions of the gene were cloned and analyzed, and all intron-exon boundaries were defined. The first of the 9 exons is untranslated. Single exons encode the signal peptide, the cysteine-rich domain in the  $\alpha$  subunit, two potential amphipathic helices flanking a heparin-binding consensus sequence, and a potential amphipathic helix overlapping a heparin-binding domain, supporting their potential functional significance in apoJ. A variety of mouse tissues constitutively express a 1.9 kb apoJ mRNA, with apparently identical transcriptional start sites utilized in all tissues tested. ApoJ mRNA was most abundant in stomach, liver, brain, and testis, with intermediate levels in heart, ovary, and kidney. The high degree of similarity between mouse and human apoJ, in structure and distribution of the gene product, gene structure, and deposition in atherosclerotic plaques, suggests that the mouse is an ideal model with which to elucidate the role of apoJ in HDL metabolism and atherogenesis.—Jordan-Starck, T. C., S. D. Lund, D. P. Witte, B. J. Aronow, C. A. Ley, W. D. Stuart, D. K. Swertfeger, L. R. Clayton, S. F. Sells, B. Paigen, and J. A. K. Harmony. Mouse apolipoprotein J: characterization of a gene implicated in atherosclerosis. *J. Lipid Res.* 1994. 35: 194–210.

**Supplementary key words** mouse apoJ • clusterin • gene structure • chromosome location • atherosclerosis

Our understanding of the proteins and processes underlying the initiation and progression of atherosclerosis remains limited, in spite of monumental efforts by basic research and clinical investigators. A major thrust of research in this area has been to provide molecular links between risk factors and the disease process. In contrast to numerous factors that predispose an individual to premature atherosclerosis, e.g., elevated levels of low density lipoproteins (LDL) and smoking, elevated levels of high density lipoproteins (HDL) appear to exert a “protective” effect as they are inversely correlated with risk (1). The genetically inbred mouse has proven to be an informative model system for dissection of the impact of specific gene products on lipoprotein metabolism, particularly that of HDL, and the pathophysiology of atherosclerosis (2–5). For example, three genes, Ath-1, Ath-2, and Ath-3, influence HDL levels and susceptibility to atherosclerosis in the mouse (2–5). This study was undertaken to determine whether the mouse model can be used to provide similar insight into the role of a recently discovered HDL-protein, apolipoprotein J (apoJ),<sup>3</sup> in atherosclerosis.

Abbreviations: apo, apolipoprotein; BSA, bovine serum albumin; CBB, Coomassie brilliant blue; CLI, complement lysis inhibitor; cM, centimorgan; Denhardt's, 50X = 1% BSA, 1% ficoll, 1% polyvinylpyrrolidone; HBD, heparin-binding domain; HDL, high density lipoproteins; HRP, horseradish peroxidase; LC, leukocyte common antigen; LDL, low density lipoproteins; PBS, phosphate-buffered saline; RFLP, restriction fragment length polymorphism; RI, recombinant inbred; SDP, strain distribution pattern; SDS, sodium dodecyl sulfate; SGP-2, sulfated glycoprotein-2; SP-40,40, serum protein 40-40; SSC, 20X = 3 M NaCl, 0.3 M sodium citrate; SSPE, 20X = 0.2 M  $\text{NH}_4\text{PO}_4\text{H}_2\text{O}$ , 0.02 M EDTA, 3 M NaCl; TxAA, transplant-associated arteriosclerosis.

<sup>1</sup>Current address: McLaughlin Research Institute, 1520 23rd Street South, Great Falls, MT 59401.

<sup>2</sup>To whom correspondence should be addressed at: Department of Pharmacology and Cell Biophysics, College of Medicine, University of Cincinnati, 231 Bethesda Avenue, Cincinnati, OH 45267-0575.

<sup>3</sup>Apolipoprotein J has also been designated clusterin, complement lysis inhibitor, glycoprotein III, glycoprotein 80, serum protein 40-40, sulfated glycoprotein-2, and testosterone repressed prostate message-2.

ApoJ, a secretory glycoprotein of vertebrates, is a component of most physiological fluids (6, 7). The function of apoJ is unknown. In human blood, apoJ, a disulfide-linked heterodimer (apoJ $\alpha\beta$ ) produced by internal cleavage of proapoJ, is associated with heterogeneous subclasses of  $\alpha$ 2-migrating HDL (8–11), suggestive of a lipid transport function. Two lines of evidence implicate apoJ's involvement in atherosclerosis. ApoJ is concentrated in adult femoral artery atherosclerotic plaques (12). In contrast, morphologically healthy adult arteries contain little or no apoJ. Platelets, which have been strongly implicated in the pathogenesis of atherosclerosis, store apoJ in  $\alpha$ -granules and release it in response to thrombin, collagen, and adenosine diphosphate activation (12, 13). No other apolipoprotein has been localized to platelets. Moreover, apoJ, present in plasma of normolipidemic individuals at a concentration of about 10 mg/dl, is positively correlated with plasma cholesterol, triglyceride, apoB, and apoE in plasma obtained from hyperlipidemic subjects (14). Thus, apoJ present in femoral artery lesions may be derived from the plasma and/or from localized platelet activation in regions of arterial damage.

The presence of apoJ in atherosclerotic plaque may augment or retard the development of these lesions, or may simply be a passive marker of vascular injury. To determine whether apoJ may have an active role in the pathogenesis of atherosclerotic plaque or in other related vascular pathologies, we have investigated its presence in other types of atherosclerotic lesions, such as in transplant-associated arteriosclerosis (TxAA) in the human heart and in diet-induced aortic valve lesions in mice. We report here that accumulation of apoJ appears to be a feature common to many types of vascular lesions associated with lipid deposition. Finding apoJ in aortic valve lesions in the diet-induced model of atherosclerosis in the mouse provides a rationale to manipulate the mouse apoJ gene as a test for its role in atherosclerosis. In order to develop this strategy we have isolated and characterized the mouse apoJ cDNA and gene and mapped the chromosomal location of the gene.

## METHODS

### cDNA library screening and sequencing

A  $\lambda$ <sub>ZAP</sub> mouse (C57BL/6  $\times$  CBA F1, female) liver cDNA library (Stratagene, La Jolla, CA) was screened ( $8 \times 10^5$  plaques) with a high-stringency hybridization solution that contained  $6\times$  SSC,  $10\times$  Denhardt's, 1% sodium dodecyl sulfate (SDS), 100  $\mu$ g/ml of sheared denatured salmon sperm DNA, and 10  $\mu$ g/ml of polyA at 65°C. The probe used was a 733 bp *Eco*RI fragment of the human cDNA clone  $\lambda$ 1–3 (15), labeled with [ $\alpha$ -<sup>32</sup>P]dATP to high specific activity by the random priming method (16), using a commercially available kit (Stratagene). In vivo

excision of plasmid DNA from the phage isolates was performed, according to the supplier's instructions, and cDNA fragments were subcloned into M13mp18 or mp19 (17) for sequencing by the quasi-end labeling adaptation of the dideoxy chain-termination method (18).

To obtain the sequence of the mouse apoJ mRNA that was missing from the 5' end of the mouse apoJ cDNA, the 5'-RACE procedure, devised by Frohman, Dush, and Martin (19) was used as modified by GIBCO/BRL (Gaithersburg, MD). Epididymal mRNA (1  $\mu$ g) was reverse-transcribed, using an apoJ-specific antisense oligonucleotide primer corresponding to nucleotides 518–537 of the deduced cDNA (see Fig. 3). First strand cDNA was C-tailed and subjected to PCR amplification, using a dI-modified polyG anchor primer (BRL) and a nested apoJ primer corresponding to the antisense complement of nucleotides 475–494 of the deduced cDNA. Upon agarose gel electrophoresis a single band of approximately 500 bp was obtained, purified, and subcloned into the PCR cloning vector pT7 (Novagen Cloning Systems, Madison, WI) for sequence analysis.

### Genomic DNA library screening and sequencing

A  $\lambda$ <sub>DASH</sub> mouse genomic library (Stratagene) prepared from DNA isolated from strain Sv129 male mice (provided by Dr. Marcia Shull, Cincinnati, OH) was screened with a human apoJ cDNA probe mixture that contained two cDNAs, a 1:1 mol ratio of a 733 and 824 bp *Eco*RI fragments that encompass the entire coding region of the mature human protein through the polyA tail (15), labeled by nick translation. Hybridization was performed overnight at 60°C in  $6\times$  SSC, 0.02 M Tris-HCl, pH 7.5,  $2\times$  Denhardt's solution, 0.5% SDS, 1 mM EDTA, 45  $\mu$ g/ml salmon sperm DNA, and 10% dextran sulfate. Filters were washed in  $2\times$  SSC/0.1% SDS at 60°C and autoradiographed overnight at  $-80^\circ\text{C}$ . Nine positive clones were obtained from a total of  $2 \times 10^6$  plaques. The DNA fragments corresponding to apoJ-hybridizable regions were subcloned into the vector pBluescript II (Stratagene) and either sequenced directly (20) or treated with Exonuclease III and mung bean nuclease to generate nested deletions (Stratagene) and then sequenced. Sequencing reactions were performed using phagemid templates, denatured in 0.2 N NaOH and heated at 65°C for 10 min, 7-deaza-2'-deoxy-5'-guanosine triphosphate, and Sequenase version 2.0 (US Biochemical, Cleveland, OH). Sequencing reaction products were electrophoresed through an 8% Sequagel (National Diagnostics, Atlanta, GA).

### Southern hybridization analysis

Mouse genomic DNA (10  $\mu$ g) prepared from strain Sv129 male mice was subjected to restriction analysis and electrophoresed through a 0.8% agarose/1 $\times$  TBE gel, using standard procedures. The DNA was depurinated, denatured, neutralized, and transferred onto Gene Screen



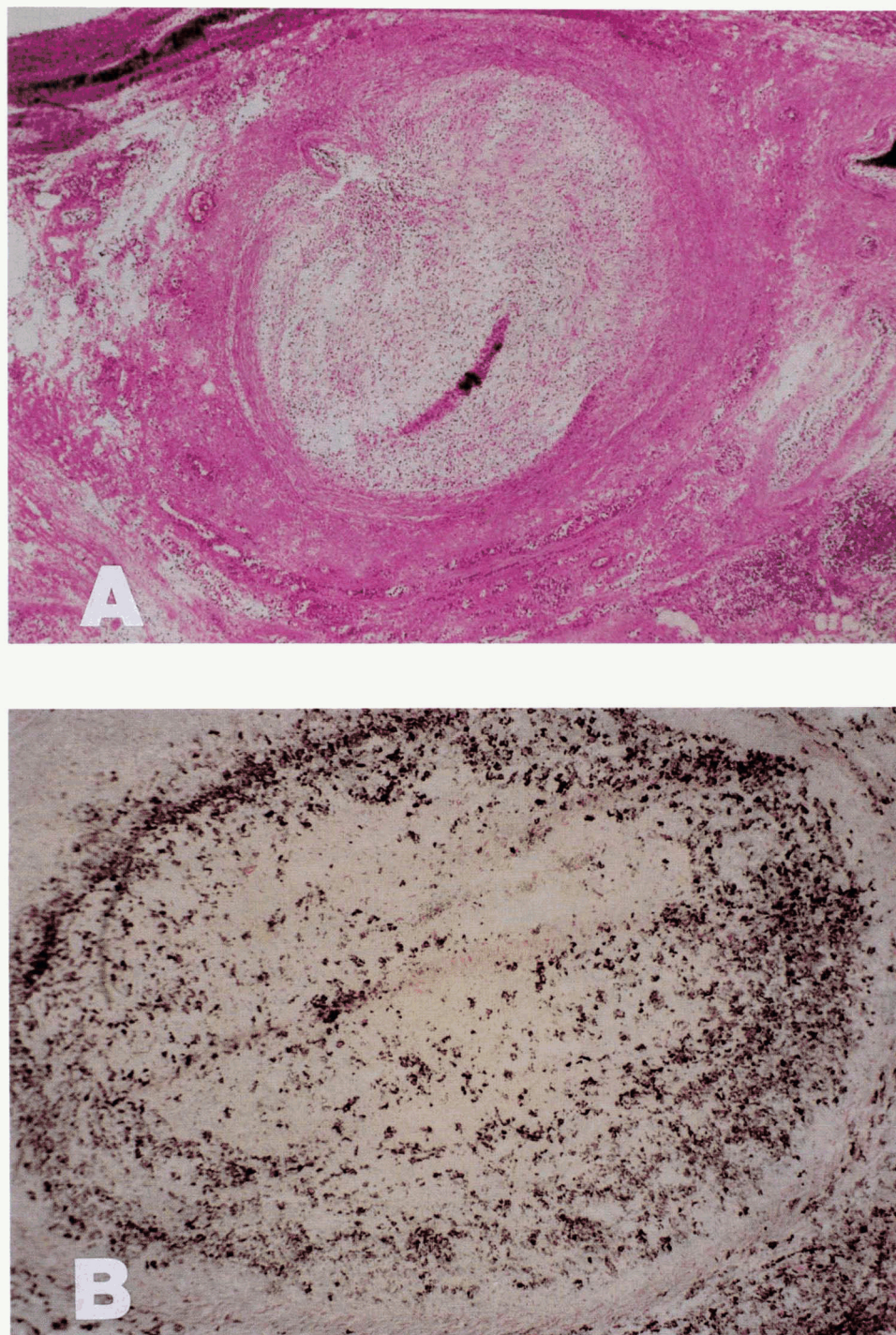
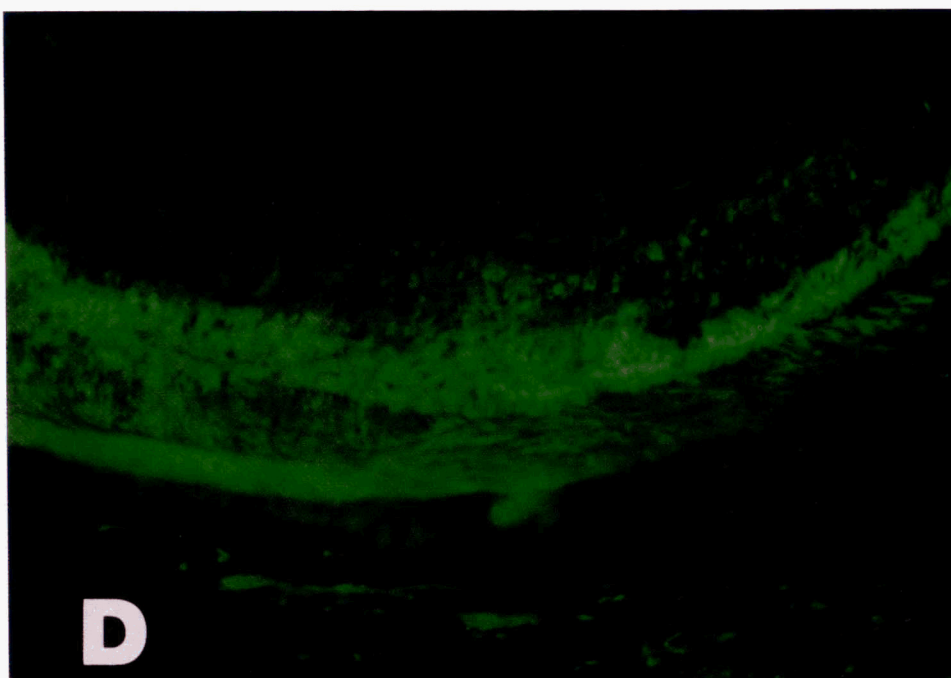
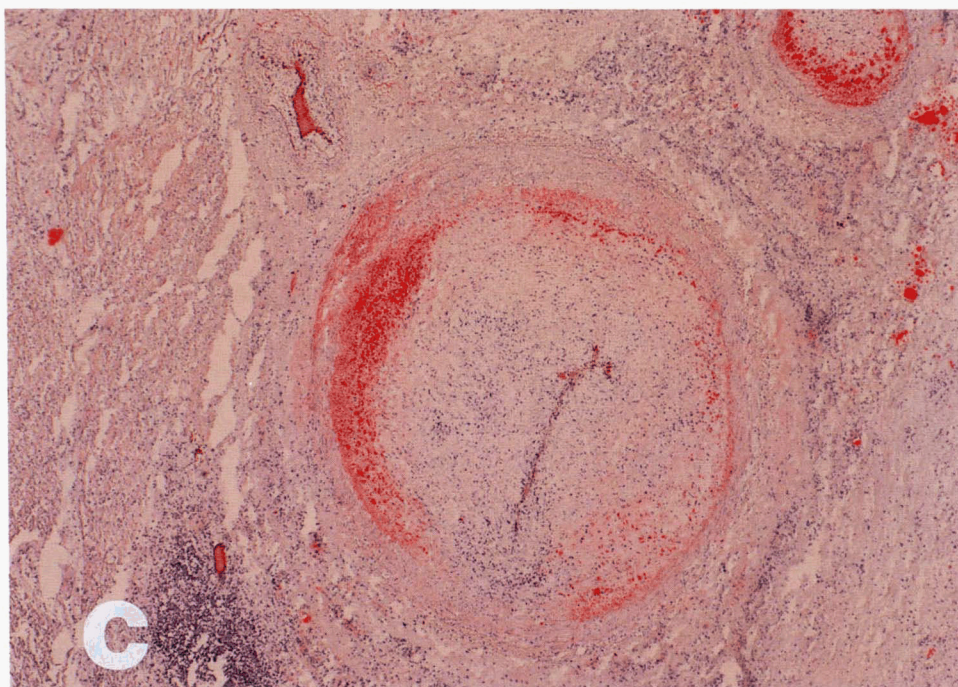


**Fig. 1.** Localization of apoJ in coronary artery plaques in transplantation arteriosclerosis. Panel A (50 $\times$ ) shows an H&E stained cross-section of a coronary artery from a patient with TxAA. The lumen is nearly obliterated by concentric intimal proliferation. Panel B (120 $\times$ ) shows immunohistochemical staining for LC in the TxAA lesion. There are numerous infiltrating mononuclear inflammatory cells in the intimal lesion. Panel C (50 $\times$ ) shows an Oil Red O stain for neutral lipids. There are focal lipid deposits that localize primarily to the interface between the intima and media. Panel D (250 $\times$ ) shows immunofluorescence for apoJ in the TxAA lesions. The distribution of apoJ protein is indicated by the green fluorescent signal. The apoJ deposition is similar to the fat deposits in the transplant lesions. This photomicrograph shows positive signal at the interface between the proliferative intima and the media and some weaker staining in the media.







Plus membrane (NEN/DuPont, Boston, MA) by capillary action, according to the manufacturer's instructions. The DNA was hybridized to mouse apoJ cDNA (clone 2-1), labeled by the random primer method (16), at 68°C in the SSC-Tris solution indicated above except the SSC was 4× concentrated. The membrane was washed in 0.1× SSC/0.1% SDS at 68°C and exposed at -80°C to Kodak (Rochester, NY) XAR-5 film, using intensifying screens.

### RNA isolation and blot hybridization analysis

Mice (A/J, C57BL/6, FVB/N) were purchased from Jackson Laboratories (Bar Harbor, ME). Swiss Webster tissues were purchased from Pel-Freez (Rogers, AR). Total RNA was extracted from mouse tissues by the modified procedure of Chomczynski and Sacchi (21), using RNAzol (BioTecx Labs, Houston, TX). RNA was quantitated by measuring its absorbance at 260 nm. RNA samples (10 µg) were denatured and then subjected to electrophoresis through a 1% agarose, 2.2 M formaldehyde gel. The integrity of the RNA was assessed from the intensity of fluorescence of ethidium bromide-stained ribosomal RNA under ultraviolet light. RNA was transferred from the gel to a Hybond-N membrane (Amersham, Arlington Heights, IL) by capillary blotting and fixed by baking at 80°C for 2 h. Prehybridization and hybridization were performed at 42°C in 50% formamide, 5× SSPE, 5× Denhardt's, 10% dextran sulfate, 0.1% SDS, and 20 µg of sheared denatured salmon sperm DNA and 10 µg/ml of polyA per ml. The probe used was an 815 bp *StuI* fragment of the mouse apoJ cDNA clone 5-1, labeled with [ $\alpha$ -<sup>32</sup>P]dATP. The filters were washed to a stringency of 0.1× SSPE/0.1% SDS at 50°C and developed. Hybridization was quantitated using a phosphorimager (Image Quant version 3.0, Molecular Dynamics, Sunnyvale, CA).

RNA dot blot analysis was performed using a filtration manifold (Bio-Rad, Rockville Center, NY). RNA samples (20 µg) were denatured in 2× SSC, 11.1% formaldehyde. Serial dilutions were applied to Hybond-N and probed with the mouse apoJ cDNA 815 bp *StuI* fragment under the same conditions used for blot hybridization.

### Primer extension analysis

PolyA<sup>+</sup> mRNA was prepared directly from whole tissue homogenates with a commercial kit, using the suggested protocol (FastTrack, Invitrogen, San Diego, CA) except for stomach mucosa, which required the use of guanidium thiocyanate (21) during initial homogenization to avoid degradation as evidenced by the integrity of ribosomal RNA bands and yield. One µg of polyA<sup>+</sup> mRNA was hybridized to 2 ng of a 5'-end-labeled (200,000 cpm) 33-mer oligonucleotide with the sequence GAGAATCTT-CATGGCGTGGCCTCCTTGGAGACT, complementary to the 5'-end of the mouse cDNA (see Fig. 3), and subjected to primer extension as described (22), using Avian

Myeloblastosis Virus reverse transcriptase (Promega, Madison, WI).

### Tissue samples and processing

Postmortem human cardiac graft tissue was obtained from a 3-year-old male cardiac transplant patient who died 2.5 years post-transplant. Mouse hearts with aortae intact were obtained from control and diet-induced (23) female C57BL/6 littermates; the mice were 10 months of age, and the induced mice had been fed a standard synthetic atherogenic diet, consisting of 50% sucrose, 15% cocoa butter, 1% cholesterol, and 0.5% sodium cholate, for 8 months. Human tissue was snap-frozen in liquid nitrogen and stored at -20°C; mouse hearts were either snap-frozen for immunohistochemistry or fixed at 4°C in paraformaldehyde, as described below, for in situ hybridization. Cryostat sections of unfixed tissues were cut at 6–8 µm and stained with hematoxylin and eosin for morphologic analysis and with Oil Red O for detection of lipid deposits. Serial sections of the mouse hearts were cut longitudinally through the aortic valve.

### In situ hybridization analysis

Fresh tissue was fixed in 4% (w/v) paraformaldehyde in PBS overnight at 4°C, then saturated in 30% sucrose in PBS overnight at 4°C before embedding in O.C.T. compound (Miles Laboratories, Elkhart, IN) and snap-frozen. Cryostat sections were cut at 6–8 microns, air-dried on slides coated with 3-aminopropyltriethoxysilane (Sigma, St. Louis, MO) and fixed for >1 h with 4% paraformaldehyde at room temperature. Prehybridization and hybridization were performed as previously described (24), using <sup>35</sup>S-rUTP-labeled antisense and sense mouse apoJ cRNAs as probes. The cRNA was transcribed from clone 5-1, using a commercially available kit (Stratagene). After hybridization and stringent wash conditions, the slides were dipped in NTB2 emulsion (Kodak), exposed for 7–10 days and developed in D19 developer (Kodak). Sections were counterstained in hematoxylin and eosin and photographed under dark- and bright-field illumination.

### Immunohistochemistry

Cryostat sections of unfixed snap-frozen tissues were obtained as described above. All sections were fixed for 10 min in acetone and then immunostained. Nonspecific binding was blocked with 5% nonfat dried milk in PBS. ApoJ protein in human tissue was localized with mouse monoclonal antibody mAb11 (12) against human apoJ, diluted 1:100. The primary antibody was detected with fluorescein-conjugated antimouse F(ab')<sub>2</sub> (Dako, Carpinteria, CA). After a 15-min incubation of the sections in 0.5% H<sub>2</sub>O<sub>2</sub> to inactivate endogenous peroxidases, apoJ protein in mouse tissue was localized by rabbit polyclonal antibody (1 µg of purified IgG/slide) raised against rat apoJ (SGP-2) (provided by Drs. Michael Griswold and

Steven Sylvester, Washington State University). The primary antibody was allowed to react with goat anti-rabbit IgG, diluted 1/25, followed by peroxidase-anti-peroxidase complex (Cappel, Durham, NC), diluted 1/100; the complex was detected with diaminobenzidine. Slides were counterstained with hematoxylin. Control slides were incubated with normal mouse serum or rabbit preimmune serum, as appropriate, and the secondary antibody.

To evaluate white blood cell infiltration into human tissue, sections were incubated for 15 min in 0.5% H<sub>2</sub>O<sub>2</sub> in methanol to quench endogenous peroxide, subjected to proteolysis in 0.1% trypsin and 0.1% CaCl<sub>2</sub> (pH 7.6–7.8) for 5 min at 37°C, washed in BSA buffer (20 mM Tris-HCl, pH 8.2, 150 mM NaCl, 0.1% bovine serum albumin (BSA)), blocked for 30 min at room temperature with 10% tissue culture grade horse serum (Hyclone, Logen, UT) in BSA buffer, and stained at 4°C for 8–20 h with mouse mAb against leukocyte common antigen (LC, Dako) diluted 1/20 in BSA buffer. LC is a 200 kDa surface marker of lymphocytes, macrophages, histiocytes, and polymorphonuclear leukocytes. Sections were rinsed thoroughly, and the primary antibody was detected with the antimouse Vectastain Elite kit (Vector Labs, Marion, IA), according to manufacturer's directions.

#### Plasma samples

Mouse blood was collected by cardiac puncture in the absence of anticoagulant or into 5 mM EDTA and put immediately on ice. Human blood was collected from healthy male donors by venipuncture in the absence of anticoagulant or into EDTA vacutainers. Cellular components were separated at 4°C by centrifugation at 2300 *g* for 15 min. Plasma was removed and centrifuged at 14,400 *g* for 10 min to remove any residual cells.

#### Electroimmunoblot analysis

For agarose electrophoresis, plasma (1–2  $\mu$ l) was loaded directly onto a 1% agarose gel (Ciba-Corning, Palo Alto, CA) and electrophoresed at 10°C and 200 V for 35 min in 50 mM barbital buffer with 1 mM Na<sub>2</sub>EDTA, pH 8.6, as reported (11). Protein was stained with 0.2% Coomassie brilliant blue (CBB); lipid was visualized with Fat Red 7B. Duplicate samples were press-blotted onto nitrocellulose (Hoefer, San Francisco, CA) and stained for apoJ with a 1/1000 dilution of mAb11 conjugated to horseradish peroxidase (HRP) (human apoJ) or with a 1/500 dilution of rabbit anti-rat-SGP-2 followed by a 1/5000 dilution of sheep anti-rabbit IgG-HRP conjugate (mouse apoJ).

For gel electrophoresis, serum samples, solubilized immediately in 10 mM Tris-HCl, pH 6.8, containing 10% glycerol, 2% SDS, and 25 mM dithiothreitol (DTT) as specified, were subjected to polyacrylamide gel electrophoresis in the presence of sodium dodecyl sulfate (SDS-PAGE), using 10% acrylamide gels (11). Electrophoresis

samples were transferred for immunostaining to nitrocellulose at 300 mA for 3 h at room temperature in transfer buffer (25 mM Tris, pH 8.3, 192 mM glycine, 20% methanol). The nitrocellulose was incubated overnight with the appropriate primary antibody (see above), typically a 1/1000 dilution in blocking buffer (50 mM Tris-HCl, pH 7.4, 150 mM NaCl, 5% nonfat dry milk, 0.01% (v/v) antifoam A, and 0.001% (w/v) merthiolate). The blots were washed thoroughly in blocking buffer, incubated for 2 h with HRP-conjugated secondary antibody (1/3000), and developed as described previously (8). Band intensities were quantitated by laser densitometry (Pharmacia LKB, Piscataway, NJ).

## RESULTS

### ApoJ in transplant-associated arteriosclerosis (TxAA)

Sections of the coronary arteries from a human cardiac graft showed severe, diffuse TxAA (Fig. 1A). The lesions were characterized by substantial intimal cell proliferation, which in one area occluded >95% of the vascular lumen. Immunohistochemistry for leukocyte common antigen (LC) showed numerous infiltrating cells in the intimal lesion (Fig. 1B). The infiltrating cells were predominantly T lymphocytes and macrophages, based on morphologic criteria and positive staining with macrophage- and T cell-specific markers (data not shown). Lipid deposits were primarily localized to the interface between the media and intimal layers (Fig. 1C). ApoJ protein, evaluated by immunohistochemistry, was colocalized with lipid at the media-intimal interface (Fig. 1D). We were unable to obtain signal by *in situ* hybridization, most likely due to mRNA degradation based on lack of signal from  $\beta$ -actin antisense probe (data not shown).

### Diet-induced atherosclerosis in the mouse

Hearts from C57BL/6 control mice and mice fed an atherogenic diet for 8 months were also examined for apoJ (Fig. 2). Shown in Fig. 2A is a section stained with Oil Red O to reveal the lipid accumulations in the aortic valve region of the heart of a mouse fed an atherogenic diet. Development of such lipid deposits is characteristic of C57BL/6 mice fed a high fat diet (2, 3). No similar lipid deposits were detected in a mouse fed a control, low fat diet (not shown). The lipid deposits in the lesions of mouse fed the high fat diet were focal and localized to the intimal layer, characteristic of an early fatty streak. ApoJ protein, detected by immunohistochemistry (Fig. 2B), was colocalized with lipid in the atherosclerotic lesions. Some of the foam cells in the lesions expressed apoJ mRNA, as determined by *in situ* hybridization analysis (Fig. 2C). ApoJ-positive cells were not present in the nonatheromatous regions of the aorta.



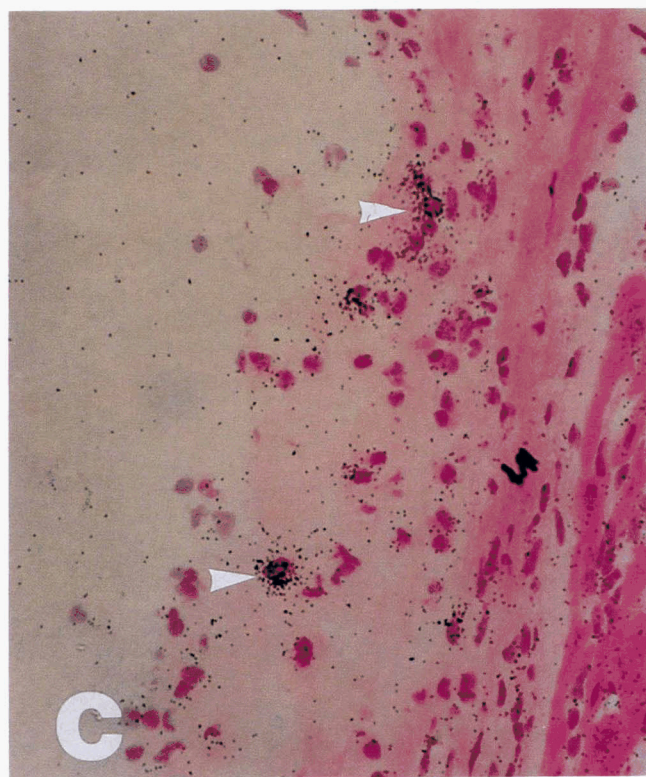
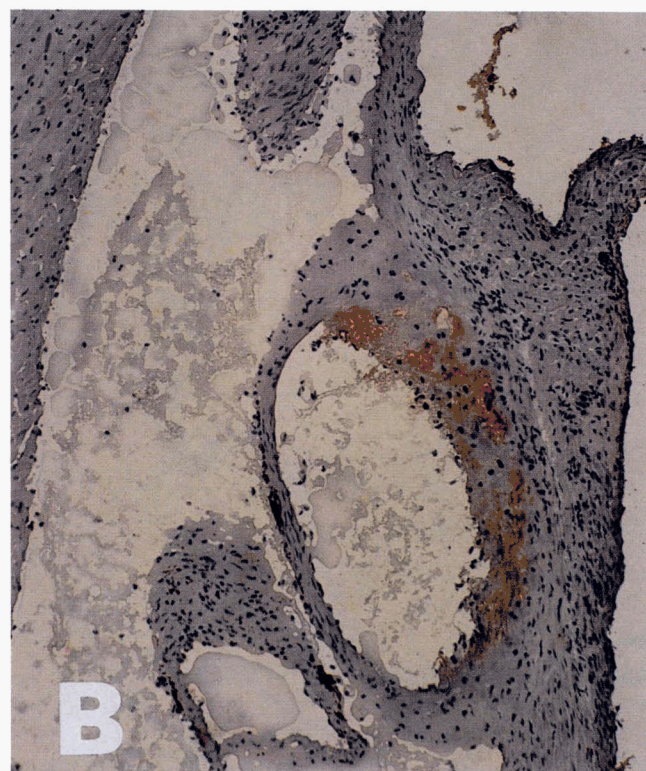
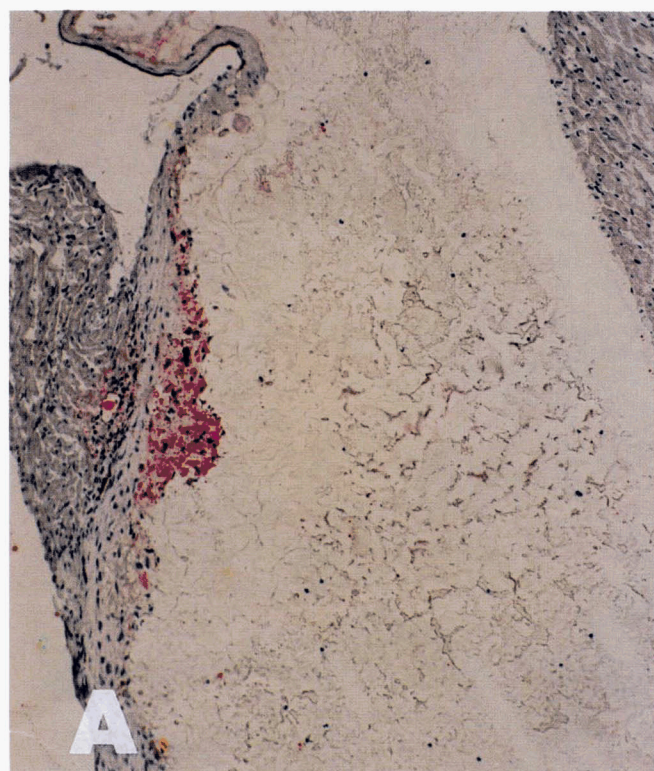


**Fig. 2.** ApoJ is present in diet-induced atherosclerotic lesions in the mouse. Panel A (120 $\times$ ) shows a section through the aortic valve region of a mouse on a high fat diet. This Oil Red O stain shows lipid deposits in the subendothelial region. Some of the lipid is contained within the cytoplasm of infiltrating cells. Panel B (120 $\times$ ) shows immunohistochemical localization of apoJ protein in the high fat diet mouse. There is focal strong signal (brown reaction product) in the subendothelial fatty lesions in the aortic valve region. Panel C (600 $\times$ ) shows localization of apoJ mRNA in the diet-induced atherosclerotic lesions by in situ hybridization. There are infiltrating cells in the atherosclerotic lesions that are strongly positive for apoJ mRNA (arrows, black grains). There is no signal present in the noninvolved areas of the aorta.





## Primary structure of mouse apoJ

Structural features responsible for apoJ's accumulation in atherosclerotic lesions in humans and mice are unknown. Important structural domains are expected to be highly conserved in mouse and human apoJ. To identify these conserved domains, we cloned and sequenced the mouse apoJ cDNA and compared it to that of human apoJ (15). A long open reading frame (ORF) was observed in the cDNA (Fig. 3), extending from nucleotide 1 to a stop codon at position 1370. An ATG at position 28 predicts a nascent polypeptide (preproapoJ) of 448 amino acids, with a calculated molecular mass of 50,260 daltons. There were 242 nucleotides of 3' noncoding sequence, with a polyadenylation consensus sequence (25) at position 1580; 27 bp of 5' noncoding sequence was represented in the cDNA. The overall nucleotide sequence identity between the mouse and human or rat cDNA is 81% versus 92%.

The deduced amino acid sequence of the mouse homolog of apoJ is also displayed in Fig. 3. The assignment of the codon used for initiation of apoJ protein synthesis, the ATG beginning at position 28 of the cDNA, was based upon comparison with both human and rat apoJ predicted start sites and the presence of a translation initiation sequence described by Kozak (26) at nucleotides -3 to +4 relative to the ATG. A 21 amino acid hydrophobic signal sequence of preproapoJ, as well as its cleavage site to produce proapoJ, was predicted by comparison to human and rat apoJ homologs. Conservation of the Arg-Ser cleavage site at position 205-206 of the proprotein predicts an  $\alpha$  subunit of 205 amino acids with a calculated molecular mass of 24,820 daltons and a  $\beta$  subunit of 222 amino acids with a molecular mass of 25,458 daltons.

The extent of overall identity of apoJ at the amino acid level between mouse and human (15, 27, 28) or mouse and rat (29) is 75% and 91%. There is more conservation within the potential functional domains (Table 1 and

TABLE 1. Comparison of amino acid sequences of putative apoJ functional domains

Species	Protein Sequence	Exon	Domain	% Homology
Mouse	MKILLLCVAMLLIWDNGMVLG	II	signal peptide	
Rat	.....L..T.....			95.2
Human	..T...F.G.L..T.E.S.Q...			66.7
Mouse	RKSLNLSLEEAKKKK	III	heparin binding	
Rat	.....			100
Human	..T..SN.....			80.0
Mouse	CNETMMALWEECKPCLKHTCMKFYARVC	IV	cysteine motif	
Rat	.....			100
Human	.....Q.....			96.4
Mouse	MQDSFARASGIIDT	V	amphipathic helix	
Rat	.....T.....			92.9
Human	...H.S...S...E			71.4
Mouse	PHKRPH	V	heparin binding	
Rat	.....			100
Human	..R...			80.0
Mouse	MFQPFPEMIHQAAQAMD	V	amphipathic helix	
Rat	.....D.....			94.1
Human	.....L....E.....			88.2
Mouse	CKEIRRNSTGCLKMKGQCEKCEILSV	VI	cysteine motif	
Rat	.....H.....			96.3
Human	..R...H.....R..D..D..R.....			78.0
Mouse	DC	VII	cysteine motif	
Rat	..			100
Human	..			100
Mouse	VSKDNPKFMDTVAEKALQ	VIII	amphipathic helix	
Rat	.....			100
Human	..RK.....E.....			83.3
Mouse	KDNPK	VIII	heparin binding	
Rat	.....			100
Human	RK...			60.0
Mouse	YRRKS	VIII	heparin binding	
Rat	.....			100
Human	..K..H			60.0
Mouse	R	IX	heparin binding	
Rat	.			100
Human	.			100

Fig. 3): the amphipathic helices, the heparin-binding domains (HBD), and the cysteine(Cys)-rich domains. The organization and spacing of the Cys residues were identical in the mouse, rat, and human apoJ homologs. The Cys domain in the  $\alpha$  subunit has the highest homology between mouse and human apoJ and significant homology to the Cys motif in C7, C8, and C9 complement components (27). In human apoJ, all of the Cys residues are used in interchain disulfide bonds (30, 31). Mouse apoJ has six potential N-glycosylation sites, two in apoJ $\alpha$  and four in apoJ $\beta$ , all of which are conserved in the rat homolog SGP-2 (21). Post-translational modification of rat apoJ utilizes all N-linked glycosylation sites for addition of carbohydrate moieties (32). Human apoJ $\alpha$  has one additional potential N-glycosylation site (15). In addition, there is a consensus glycosaminoglycan site, SGSG at residue 115 of the proprotein, that is conserved in mouse, rat and human apoJ (6).

#### Mouse plasma apoJ

To determine whether apoJ is, as human apoJ, a plasma protein, mouse and human plasma were assayed for apoJ by electroimmunoblot analysis. ApoJ was detected in mouse plasma. By SDS-PAGE (Fig. 4A) under nonreducing conditions, the  $M_r$  values of mouse and human apoJ were similar, 73 and 78 kDa, respectively. Duplicate samples were reduced prior to analysis to determine whether

mouse apoJ is, like human apoJ, predominantly a heterodimer. Mouse apoJ was reduced to two subunits, indicating cleavage of proapoJ; however, mouse apoJ subunits differed from human apoJ subunits in apparent  $M_r$ . Human apoJ $\alpha$  and apoJ $\beta$  are, as previously reported (8), similar in size ( $\sim 37$  kDa). The mouse subunits, in contrast, were 32 and 41 kDa. One mouse apoJ subunit is likely to be more heavily glycosylated than the other. Alternatively, mouse proapoJ cleavage may not occur at the predicted Arg-Ser bond. SDS-PAGE/electroimmunoblot analysis was also used to compare the abundance of plasma apoJ in different strains of mice. The level of apoJ was approximately 3 times higher in C57BL/6 compared to A/J mice; apoJ levels present in plasma obtained from FVB/N mice were roughly equivalent to those in C57BL/6 mice. There was little ( $\pm 10\%$ ) variation in apoJ level between individual mice of the same strain.

The distribution of apoJ in mouse versus human plasma, relative to that of the lipoprotein classes, was compared by agarose electrophoresis under nondenaturing conditions. CBB stain for protein revealed distinct patterns for mouse and human plasma proteins separated by agarose gel electrophoresis (Fig. 4B). Based on the lipid stain, the majority of mouse lipid migrated in the  $\alpha 1$  region, equivalent to human HDL. This is expected as HDL is the predominant mouse lipoprotein (5). Mouse apoJ migrated slightly faster than human apoJ ( $\alpha 1$  vs.  $\alpha 2$

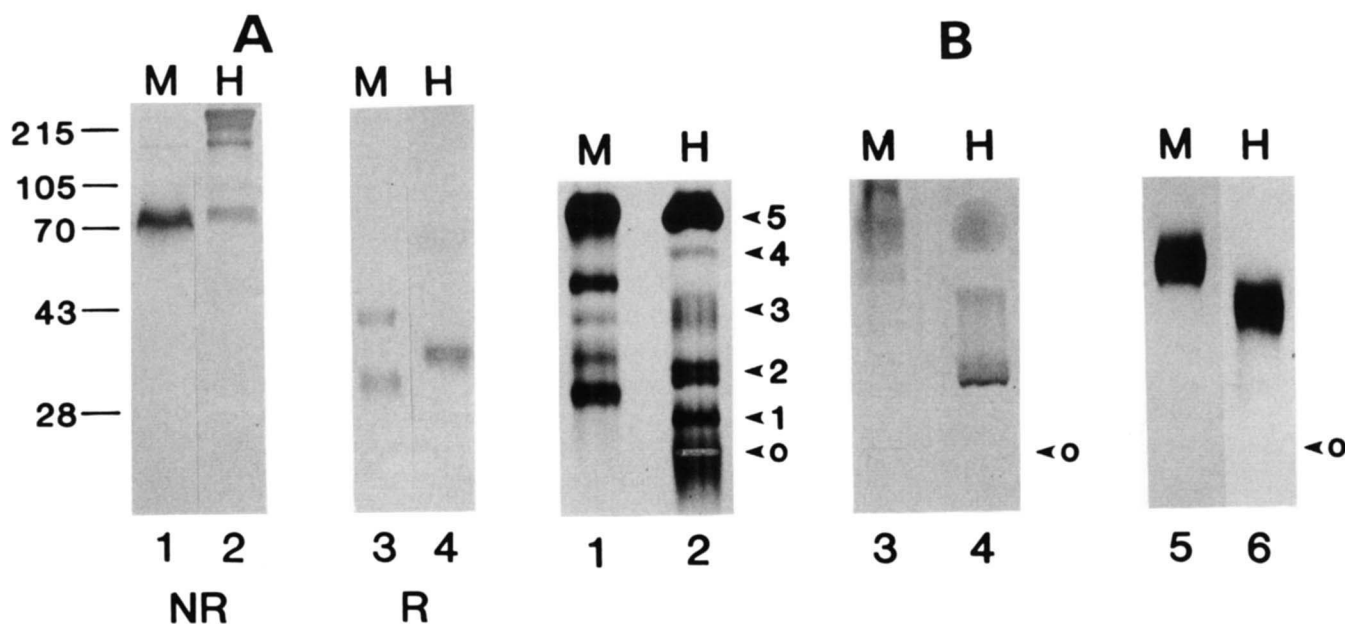


**Fig. 4.** Comparison of mouse and human plasma apoJ. A: For SDS-PAGE analysis, 1.5  $\mu$ l of mouse (M) and 0.2  $\mu$ l of human (H) serum were subjected to SDS-PAGE and electroimmunoblotting, as described in Methods; the positions and  $M_r$  values (kDa) of prestained molecular weight markers (Bethesda Research Laboratories) are indicated. Lanes 1 and 2 are mouse and human serum electrophoresed under nonreducing conditions; lanes 3 and 4 are mouse and human serum, in the presence of 25 mM DTT. Lanes 2 and 4 were stained with rabbit anti-apoJ; lanes 1 and 3, with rabbit anti-SGP-2. The secondary antibody was sheep anti-rabbit IgG-HRP conjugate. B: Mouse (M) and human (H) plasma were subjected to agarose electrophoresis, as described in Methods. Lanes 1 and 2 were stained with CBB; the positions are labeled as 0, origin; 1, fibrinogen; 2, transferrin ( $\beta_1$ ); 3,  $\alpha 2$ -macroglobulins; 4,  $\alpha 1$ -antitrypsin; 5, albumin. Lanes 3 and 4 were stained with Fat Red 7B; in human plasma, HDL migrated the furthest followed by VLDL and LDL, respectively. Lane 5 was stained with rabbit anti-SGP-2 followed by sheep anti-rabbit IgG-HRP conjugate; and lane 6, with mAb11-HRP conjugate.



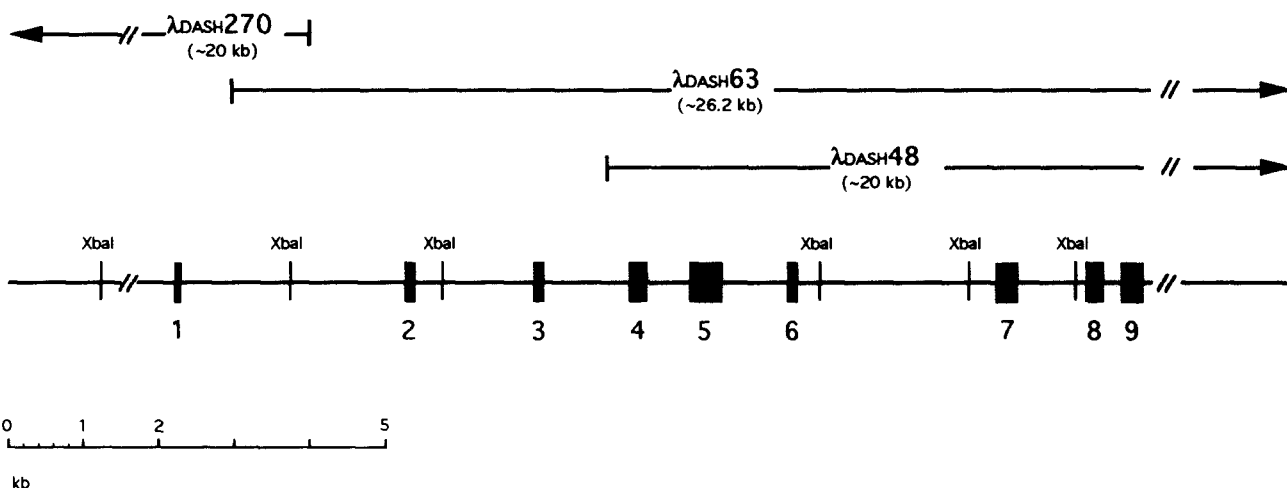


Fig. 5. The mouse apoJ gene. The overlapping  $\lambda$ DASH clones are shown (top) with the exon-intron organization of the coding segment of the gene indicated (bottom). The rectangles represent exons; the horizontal line indicates introns. The exon numbers are given below the rectangles.

mobility), suggesting that the majority of mouse apoJ is associated with the bulk of the HDL.

#### Analysis of the mouse apoJ gene

As a prerequisite to manipulating the apoJ gene in the mouse, and as an alternative approach to identifying potential apoJ functional domains, the gene was cloned and sequenced. Based on Southern blot analysis, the size of the mouse apoJ gene was determined to be approximately 23 kb (data not shown). Seven apoJ genomic clones were isolated from a mouse genomic library, and three of these ( $\lambda$ DASH48,  $\lambda$ DASH63, and  $\lambda$ DASH270) were used to determine the intron/exon junctions and to map the position of the exons within the gene (Fig. 5). The complete apoJ gene is composed of 9 exons. The 5' and 3' splice donor and acceptor sequences conform to the GT/AG consensus sequences. Exon I (Fig. 6) contains the 5'-untranslated region (UTR). Exon I was identified by

sequencing the RACE clone and confirmed by primer extension sequencing, using mouse mRNA isolated from Sertoli cells, primer extended from an oligonucleotide complementary to a region within Exon III. Exons II-V encode the  $\alpha$  subunit. The  $\beta$  subunit is encoded within Exons V through the first part of Exon IX. The 3'-UTR, including sequence through the polyadenylation signal of mouse apoJ cDNA, is also contained within Exon IX. The exons range in size from 45 to 412 bp (Table 2). The largest exon, Exon V, spans the  $\alpha/\beta$  cleavage site. The introns range in size from 257 bp to >3 kb. Comparison of the exonic organization of the mouse apoJ gene with those of the rat (33) and human (MacVector, version 2; GenBank, release 71) genes (Table 2) indicates a high degree of structural conservation. In the case of the mouse apoJ gene, the exonic sequences are identical to the cDNA with five exceptions, all in the 5' portion of the cDNA (Fig. 3). In the 5' UTR, three differences were found at

Gene	CATGCGCCCCCTGGTGCCCCCGCTGGGTGCTGCGCCTCTTACCCCCACCTCTAGGCTTC	-123
	CAGAAAGCTCCTGGTGATTCTCCGGCATTCTCTGGGCGTGAGTCACGCAGGTTTGCAGC	-63
	CAGCCCCAAAGGGGTGTACTTGAGCAGAGCGC <u>TATAAAT</u> AGGGCGCTTCCCCGGTGCTCA	-3
	1 2	
	↓ ↓	
	CC <b>ACCCGCGTCACCAGGAGGAGCGCACTGGAGCCAAGCCGCAGACCGGTGAGA</b>	51
	.CN.....N.....A.....	43*
	CAGCTGCACCTTTACTACCCCAGACNCGNAGCCACACGCAGATGCAGGCAGGTAGCAGC	110
	TAGTGAAC TG	120

Fig. 6. Exon I and 5' flanking sequence. Exon I, shown in bold type, was identified by sequencing the RACE clone. The asterisk (\*) represents the reverse transcribed, polymerase chain reaction amplified RACE product. The TATA box consensus sequence, indicated in italics, is underlined. The splice donor consensus sequence is indicated by the double underline. The 5' ends of the two primer extension products (Fig. 8) of mRNA from mouse Sertoli cells are indicated by the arrows as 1 and 2.

TABLE 2. Exonic organization of the apoJ gene

Species	Exon	cDNA Position <sup>a</sup>	Length (bp)	Splice Donor	Splice Acceptor	% Exonic Homology	Domain	cDNA Position
Mouse	I	N/A <sup>b,c</sup>	45		...AGACCGgtg			
Rat		–10–35 <sup>d</sup>	45		...AGACCGgtg	97.8		
Human		N/A <sup>b,e</sup>	47		...TGACCGgtg	61.7		
Mouse	II	1–121	121	ttgcagGACTCC	...TCCAAGgta		signal peptide	28–89
Rat		36–156	121	ttgcagGACTCC	...TCCAAGgta	94.2		
Human		167–292	126	ctgcagAGGCGT	...TCCAGGgta	58.7		
Mouse	III	122–270	149	ccacagAACTGT	...AAAGAGgta		HBD	222–266
Rat		157–305	149	ccacagAACTGT	...AAAGAGgta	96.0		
Human		293–441	149	ttgcagAAATGT	...AAAGAGgtc	87.9		
Mouse	IV	271–441	171	ctgaagGATGCT	...CAGCAGgtg		Cys motif	327–410
Rat		306–476	171	ctgaagGGTGCT	...CGCCAGgtg	93.2		
Human		442–612	171	ctgtagGATGCC	...CGCCAGgtg	82.4		
Mouse	V	442–853	412	tcccagCTAGAG	...TAAGAGgtt		2 amph helices/1 HBD	549–800
Rat		477–888	412	tcccagCTAGAG	...TAAAAGgtc	85.2		
Human		613–1024	412	gtccagCTTGAG	...TACGAGgtg	77.9		
Mouse	VI	854–958	105	gtccagAAGGTG	...CTGTGGgtg			
Rat		889–993	105	gtccagAAGGTG	...CTGTGGgtg	93.4		
Human		1025–1129	105	ccccagAAGGCG	...CTGTGGgtg	87.6		
Mouse	VII	959–1192	234	gggcagACTGTT	...CCGTGAgtg			
Rat		994–1224	231	ggcagaACTGTT	...CAGTGAgtg	90.3		
Human		1130–1363	234	gggcagACTGTT	...CGGTGGgtg	82.9		
Mouse	VIII	1193–1364	172	ctctagCCACCC	...AAAGCCgta		1 HBD/1 amph helix	1290–1362
Rat		1225–1396	172	aggtgaCAACCC	...AAGCCGgta	94.8		
Human		1364–1535	172	aggtggCTTCCC	...GCACCCgta	80.2		
Mouse	IX	1365–1600	236	tttcaaTGCGGA	...CGATACgtg			
Rat		1397–1627	231	ttccagCATGGA	...CCTTGCgta	82.3		
Human		1536–1651	116 <sup>f</sup>	tttcagGGAGGA	...GAGCTGatc	<65 <sup>f</sup>		

<sup>a</sup>Nucleotide position in the cDNA sequence.

<sup>b</sup>N/A not available because the cDNA sequence is incomplete at the 5'-end.

<sup>c</sup>Position based on mouse cDNA sequence presented in this paper.

<sup>d</sup>Rat information obtained from the rat TRPM2 cDNA sequence in GENBANK (Release 71.0).

<sup>e</sup>Human information obtained from the human TRPM2 cDNA sequence in GENBANK (Release 71.0).

<sup>f</sup>cDNA is incomplete at the 3'-end. Homology is much less than 65% when exonic size is considered.

positions 2, 9, and 10. In the portion encoding the signal peptide, the sequence CA at positions 54, 55 of the cDNA was reversed in the gene, changing the amino acid at position 10 of preproapoJ from Met to Leu. As Leu is present at this position of rat and human preproapoJ (Table 1), we suspect that we erred in sequencing the cDNA.

### Chromosomal mapping of apoJ

Because knowledge of the chromosomal location of a gene can facilitate genetic studies and correlations, the apoJ gene was mapped by analysis of recombinant inbred (RI) mouse strains (2, 3). Mouse DNAs from several inbred strains were analyzed for the presence of restriction fragment length polymorphisms (RFLPs) within the mouse apoJ structural gene, using the mouse apoJ cDNA as probe. An RFLP was identified, using the restriction enzyme *HhaI*, displaying a 2450 bp fragment in A and AKR strains and a 3100 bp fragment in C3H, C57L, and

DBA/2 strains (data not shown). This RFLP was used to type DNA from two RI sets, AKXD (AKR×DBA/2, 25 strains) and AKXL (AKR×C57L, 18 strains). A total of 43 RI strains were typed for the *HhaI* RFLP and the strain distribution patterns (SDPs) for apoJ are shown in Table 3. Comparison of SDPs from previously typed loci for these RI sets revealed that apoJ is closely linked to Mtv-11, a mouse mammary tumor provirus (34). Two RI strains in the AKXD RI set were heterozygous for the polymorphism and were not used in the linkage analysis. The absence of recombinants between Mtv-11 and apoJ among 41 RI strains indicates (35) a distance of 0 cM (95% confidence limits 0–2.5 cM) between the two markers. The presence of two recombinants between apoJ and Rib-1 among 18 RI strains provides a map distance between these two genes (36, Table 3) of 3.3 cM with a standard error of 2.7 cM (95% confidence limits 0.4–18.1). We suggest that the RFLP determines the structure of apoJ and we designate the mouse gene *Apoj*.



TABLE 3. Strain distribution pattern of apoJ and other loci on chromosome 14 in RI strains derived from AKR and DBA or AKR and C57L

		AKXD																							
Gene		1	2	3	6	7	8	9	10	11	12	13	14	15	16	18	20	21	22	23	24	25	26	27	28
Mtv-11		D	D	A	D	A	D	A	D	A	D	A	A	D	A	D	A	A	A	A	D	U	D	A	D
ApoJ		D	D	A	D	A	D	A	D	A	D	A	A	U	A	D	A	A	A	A	D	U	D	A	D

A, genotype found in the AKR parent; D, genotype found in the DBA parent; U, untyped strains.

		AKXL																	
Gene		5	6	7	8	9	12	13	14	16	17	19	21	24	25	28	29	37	38
Mtv-11		A	A	A	L	L	A	A	A	L	L	L	A	A	L	L	L	A	A
ApoJ		A	A	A	L	L	A	A	A	L	L	L	A	A	L	L	L	A	A
Rib-1		A	A	A	L	L	A	A	x L	L	L	L	A	A	L	L	L	x L	A

A, genotype found in the AKR parent; L, genotype found in the C57L parent. An x indicates a crossover event.

### Size and tissue distribution of mouse apoJ mRNA

To evaluate the relative tissue distribution of the apoJ message in the adult mouse, total RNA was isolated from various tissues and analyzed with the mouse apoJ cDNA probe. The results, shown in **Fig. 7A**, indicated that apoJ mRNA is present in a wide variety of tissues in varying amounts. Phosphorimage analysis of both Northern and dot blots (**Fig. 7B**) revealed this relative order of abundance of apoJ mRNA: stomach, liver, brain>testis, heart>kidney, ovary>spleen>submaxillary gland, thymus>thyroid. No apoJ mRNA was detected in the intestine or lung by either method. A similar pattern of tissue distribution was seen for human apoJ and rat SGP-2 among the tissues analyzed (15, 29).

### Primer extension analysis

To determine the relative position of the transcriptional start site(s) in the mouse apoJ gene utilized in different tissues, a primer complementary to the 5' end of the cDNA clone was synthesized and subjected to primer extension analysis. The vast majority of extended product corresponded to start sites at two adjacent nucleotides, generating extension products of 84 and 85 nucleotides in total size (**Fig. 8**). Thus, the primer extension product included 34 or 35 bases that extended beyond the 5' end of the largest cDNA clone. Comparing the different tissue sources of RNA, differences were observed in the relative amount of each start site product that occurred. Approximately equal amounts of the two primer extension prod-

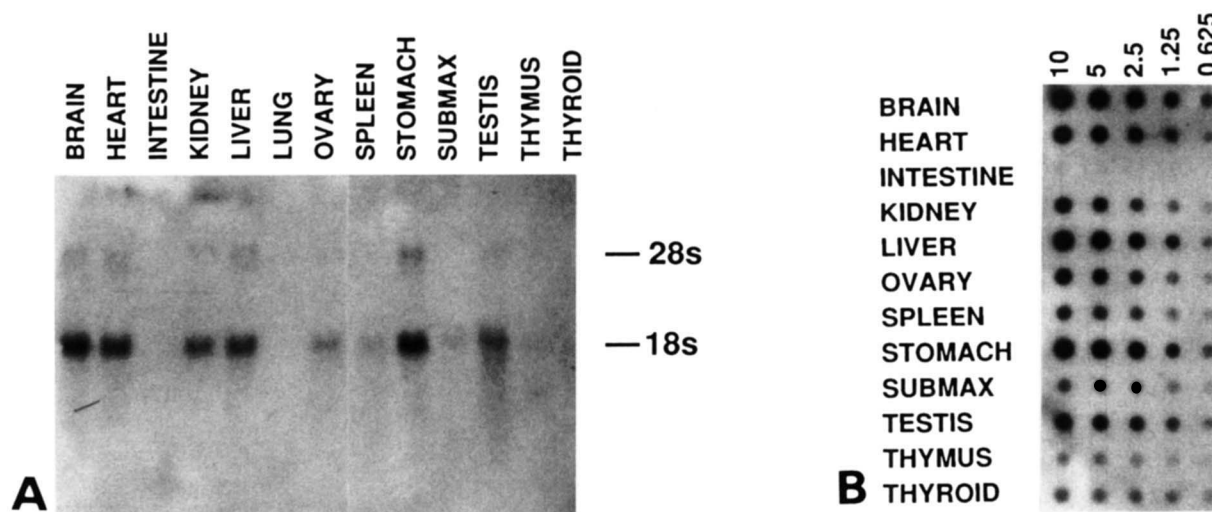


**Fig. 7.** Analysis of the distribution and abundance of apoJ mRNA in mouse tissues. **A:** Total RNA (10  $\mu$ g) from mouse tissues was subjected to electrophoresis, transferred to Hybond-N, and hybridized with radiolabeled mouse apoJ cDNA (815 bp *Stu*I fragment). The 18S and 28S ribosomal markers were detected by ethidium bromide staining of the gel. The size of the mouse apoJ mRNA is 1.9 kb. **B:** Serial dilutions of total RNA from mouse tissues (left to right in  $\mu$ g, 10, 5, 2.5, 1.25, 0.625) were applied to Hybond-N, and hybridized with the same mouse apoJ cDNA fragment as in (A). When individual dots were analyzed using a phosphorimager, each twofold dilution of RNA gave a corresponding twofold decrease in exposure density.

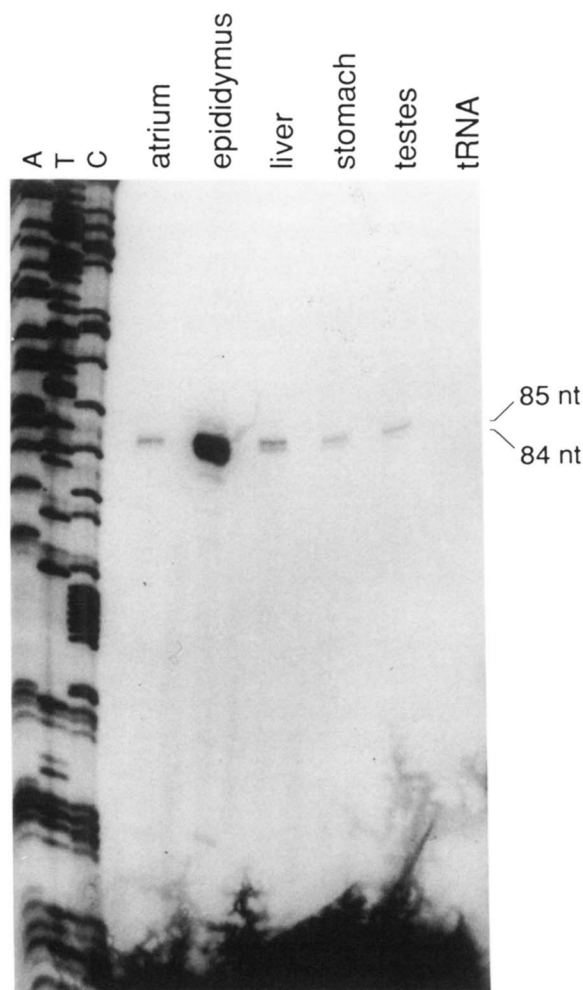


**Fig. 8.** Primer extension analysis. The relative position of the transcriptional start site(s) utilized by the mouse apoJ gene are very similar in different tissues. One  $\mu\text{g}$  of polyA<sup>+</sup> mRNA from the indicated tissues was hybridized to a 5' end-labeled oligonucleotide complementary to the 5' end of the mouse cDNA. Size standard is sequencing ladder from a Bluescript SK<sup>+</sup> vector (Stratagene), using the M13-20 forward primer. Extension products of 84 or 85 nucleotides total size represent the vast majority of the total.

ucts were present in epididymis, but the other tissues tended to have either slightly or much more of the 85-base primer extended product.

## DISCUSSION

ApoJ accumulates in atherosclerotic plaque (12) and, as reported here, in transplant-associated arteriosclerosis in humans and in aortic valve atheromatous lesions in fat-fed mice. As the pathogenesis of these two types of vascular lesions is distinct, apoJ deposition may be a general marker for arterial degeneration associated with lipid deposition. As a prerequisite to elucidating the role of

apoJ in the pathogenesis of atherosclerosis in the mouse model, we characterized mouse apoJ. The relative level of apoJ in the plasma of two strains of mice is qualitatively related to the genetic susceptibility to diet-induced atherosclerosis, decreasing in the order C57BL/6 > A/J. The susceptibility of FVB/N mice has not been tested. Both mouse and human plasma apoJ are associated with HDL. In contrast to human apoJ-HDL, however, which have  $\alpha_2$  electrophoretic mobility, mouse apoJ-HDL migrate with the bulk of the HDL in the  $\alpha_1$  position. In both mouse and human, proapoJ is cleaved to apoJ $\alpha\beta$ , which is present in the plasma. Moreover, the primary structure of mouse apoJ is 75% homologous to that of human apoJ. Based on the amino acid sequence deduced from the cDNA, mature mouse apoJ, like human apoJ, contains 427 amino acids and is synthesized with a 21-residue signal peptide. Comparison of the deduced amino acid sequence of mouse apoJ with the amino terminal sequences of the mature subunits of human apoJ (15) and rat SGP-2 (29) suggests that the apoJ subunits in these species are similarly produced by cleavage at residues 205-206 of proapoJ, with differences in apparent  $M_r$  predicted to be due to species differences in glycosylation. The high degree of similarity in structure, plasma distribution, and tissue distribution between human and mouse apoJ and the presence of apoJ deposits in human and mouse atherosclerotic lesions suggests a common function of apoJ in atherosclerosis and justifies the dissection of apoJ function in the mouse model.

ApoJ appears to be encoded by a single gene in all species examined (15, 28, 29). In the mouse, the apoJ gene is distinct from two genes correlated with atherosclerosis susceptibility in the mouse, Ath-1 and Ath-3 (2, 3), which map to chromosomes 1 and 7, respectively. RI strain analysis shows that apoJ is located on mouse chromosome 14. None of the 41 RI strains tested was discordant with the SDP of Mtv-11, a locus previously mapped to chromosome 14, indicating that apoJ and Mtv-11 are tightly linked. Using different RI strains, Birkenmeier et al. (37) also localized the mouse apoJ gene to chromosome 14. Other mouse apolipoprotein genes (apoA-I, apoA-II, apoE, apoB, apoC-I, and apoC-II) are also located on chromosomes that are distinct from the chromosomal position of apoJ (5). Human apoJ has been mapped to chromosome 8 (38). The rat homolog of apoJ (SGP-2) has not been mapped. The apoJ gene is transcribed in a variety of tissues in vertebrate species, including the mouse as reported here. In all mouse tissues examined, transcription is similarly initiated, based on primer extension analysis. The 1.9 kb apoJ mRNA detected in mouse tissues is most abundant in stomach, liver, brain, and testis. Intermediate levels of message are present in heart, kidney, and ovary; low levels are present in spleen, submaxillary gland, and thymus, and very low levels in thyroid. No apoJ mRNA is detected in the adult intestine and lung by




Northern blot or dot blot analysis. Within these expressing tissues in the mouse, the mRNA is restricted largely to cells that line fluid compartments (39), consistent with apoJ's secretory character.

The apoJ localized in atheromatous lesions may be derived from the plasma, from platelet deposition and activation (12), or from local synthesis by arterial wall foam cells. The gene is inactive in the various cell-types present in long-standing femoral artery atherosclerotic plaques (13). Although we were unable to evaluate arterial plaque in TxAA for localized apoJ gene transcription due to RNA degradation, foam cells derived from macrophages and/or smooth muscle cells in aortic valve lesions of mice fed high-fat diets do express the apoJ gene. Thus, multiple mechanisms can account for the deposition of apoJ in atheromatous lesions. Functional domain analysis of apoJ can provide insight into the mechanism of its accumulation in atherosclerotic lesions. Two types of apoJ sequences are of particular interest: 1) the heparin-binding consensus sequences, comprised of clusters of positively charged amino acid residues thought to be important in the interaction of proteins with negatively charged macromolecules (40); and 2) the amphipathic helices, found in lipid transport and hydrophobe-binding macromolecules (41, 42). These domains are likely determinants of tissue localization of apoJ. The Cys-rich motifs, found in coagulation factors and in some members of the terminal complement cascade (43), appear to be primarily apoJ structural determinants. Analysis of the gene organization substantiates the potential functionality of these domain types. A heparin-binding domain is encoded by Exon III. A heparin-binding domain and amphipathic helices flanking it on either side are encoded by Exon V, and an amphipathic helix overlapping and flanked by heparin-binding domains are encoded by Exon VIII. The arrangement of the heparin-binding and amphipathic helix motifs, as well as the apoJ $\alpha$  Cys motif, within exons strongly suggests that these protein domains are functionally significant. In contrast, the apoJ $\beta$  Cys motif, a putative nucleotide binding site, and a glycine-rich motif, suggested by Tsuruta et al. (44) to have functional significance, are each encoded by more than one exon and may therefore lack specific function.

We propose that apoJ utilizes its heparin-binding determinants to localize in the arterial wall where it utilizes its amphipathic helix domains under adverse conditions to limit arterial wall damage or to facilitate repair, rather than to augment tissue destruction. ApoJ's association in plasma with "protective" classes of plasma lipoproteins, the HDL, argues for a protective and/or repair role. Protection by HDL against atherosclerosis and coronary heart disease has been attributed to several mechanisms (45, 46), including the ability of HDL to transport extrahepatic cholesterol to the liver for biliary excretion and to facilitate removal of potentially atherogenic chylomicron

remnants by enhancing catabolism of triglyceride-rich lipoproteins. In the case of apoJ-HDL, there is the alternative possibility that anti-atherogenicity is due to inhibition of complement-mediated cell damage in the arterial wall. Prior to the discovery of apoJ and its HDL association by de Silva et al. (8), apoJ was identified in plasma in association with the soluble complement complex C5b-9 (27, 28). ApoJ is a potent inhibitor of complement-mediated cell lysis in vitro (28), giving functional significance to the apoJ/C5b-9 association. Complement has been implicated in the pathogenesis of atherosclerotic plaques (47-49). C5b-9 complexes, the terminal reaction product of the complement cascade, accumulate in plaques (50-52) and can augment lesion formation by altering the properties of arterial wall cells through cell signalling mechanisms (53) or by producing transmembrane pores.

A protective role of apoJ in the arterial wall is consistent with the cell type-specific pattern of constitutive apoJ expression (39) and its induction in types of tissue injury other than atherosclerosis. ApoJ levels are dramatically increased in other models of inducible tissue damage and degeneration, including cell death initiated by hormonal stimuli in prostate regression (54), pressure insult that occurs during renal atrophy after ureteral obstruction (55), developmental stimuli responsible for necrosis of interdigital tissue (56), and cytotoxic injury in chemotherapeutic induction of tumor regression (56). ApoJ mRNA is also increased in the brains of Alzheimer's patients and scrapie-infected hamsters, both neurodegenerative disorders (57, 58). The role of apoJ as a hydrophobe-binding, cytoprotective protein is a reasonable way to account for its constitutive and inductive patterns of expression and localization. Enhanced lipid binding and transport potential due to increased levels of apoJ would allow redistribution and/or recycling of membrane-active cellular lipid, available as a result of focal tissue destruction. Regulation of cytolytic complement function by apoJ would limit further tissue degeneration. Future studies are aimed at using the mouse as a model system to examine the cytoprotective hypothesis, particularly with respect to apoJ's role in atherosclerosis, emphasizing the manipulation of the apoJ gene in gene-targeted transgenic mice, a powerful strategy for the functional analysis of a gene product in atherosclerosis (59-64). 

T. C. Jordan-Starck and S. D. Lund contributed equally to this report. This research was supported by grants HL-41496 (Program of Excellence in Molecular Biology of the Heart and Lung) from the National Institutes of Health, and a Basic Research grant from the March of Dimes Birth Defects Foundation 1-0346 (BJA). SDL was the recipient of a postdoctoral fellowship from the NIH Training grant HL-07382. We are grateful to Ms. Kathy Saalfeld for her expert technical assistance, and to Drs. Michael Griswold and Steven Sylvester (Washington State University, Pullman, WA) for rabbit antiSGP-2.

*Manuscript received 12 October 1992 and in revised form 9 September 1993.*

## REFERENCES

1. Miller, N. E. 1987. Associations of high-density lipoprotein subclasses and apolipoproteins with ischemic heart disease and coronary atherosclerosis. *Am. Heart J.* **113**: 589-597.
2. Paigen, B., D. Mitchell, K. Reue, A. Morrow, A. J. Lusis, and R. C. LeBoeuf. 1987. Ath-1, a gene determining atherosclerosis susceptibility and high density lipoprotein levels in mice. *Proc. Natl. Acad. Sci. USA.* **84**: 3763-3767.
3. Paigen, B., M. N. Nesbitt, D. Mitchell, D. Albee, and R. C. LeBoeuf. 1989. Ath-2, a second gene determining atherosclerosis susceptibility and high density lipoprotein levels in mice. *Genetics.* **122**: 163-168.
4. Stewart-Phillips, J. L., J. Lough, and E. Skamene. 1989. Ath-3, a new gene for atherosclerosis in the mouse. *Clin. Invest. Med.* **12**: 121-126.
5. Lusis, A. J. 1988. Genetic factors affecting blood lipoproteins: the candidate gene approach. *J. Lipid Res.* **29**: 397-429.
6. Jordan-Starck, T. C., D. P. Witte, B. J. Aronow, and J. A. K. Harmony. 1992. Apolipoprotein J: a membrane policeman? *Curr. Opin. Lipidol.* **3**: 75-85.
7. Jenne, D. E., and J. Tschopp. 1992. Clusterin: the intriguing guises of a widely expressed glycoprotein. *TIBS.* **17**: 154-159.
8. de Silva, H. V., W. D. Stuart, C. R. Duvic, J. R. Wetterau, M. J. Ray, D. G. Ferguson, H. W. Albers, W. R. Smith, and J. A. K. Harmony. 1990. A 70-kDa apolipoprotein designated apoJ is a marker for subclasses of human plasma high density lipoproteins. *J. Biol. Chem.* **265**: 13240-13247.
9. James, R. W., A.-C. Hochstrasser, I. Borghini, B. Martin, D. Pometta, and D. Hochstrasser. 1991. Characterization of human high density lipoprotein-associated protein, NA1/NA2. *Arterioscler. Thromb.* **11**: 645-652.
10. Jenne, D. E., B. Lowin, M. C. Peitsch, A. Böttcher, G. Schmitz, and J. Tschopp. 1991. Clusterin (complement lysis inhibitor) forms a high density lipoprotein complex with apolipoprotein A-I in human plasma. *J. Biol. Chem.* **266**: 11030-11036.
11. Stuart, W. D., B. Krol, S. H. Jenkins, and J. A. K. Harmony. 1992. Structure and stability of apolipoprotein J-containing high density lipoproteins. *Biochemistry.* **31**: 8552-8559.
12. Witte, D. P., B. J. Aronow, M. L. Stauderman, W. D. Stuart, M. A. Clay, R. A. Gruppo, S. H. Jenkins, and J. A. K. Harmony. 1993. Platelet activation releases megakaryocyte-synthesized apolipoprotein J, a highly abundant protein in atheromatous lesions. *Am. J. Pathol.* **143**: 763-773.
13. Tschopp, J., D. E. Jenne, S. Hertig, K. T. Preissner, H. Morgenstern, A.-P. Sapino, and L. French. 1993. Human megakaryocytes express clusterin and package it without apolipoprotein A-I into  $\alpha$ -granules. *Blood.* **82**: 118-125.
14. Jenkins, S. H., W. D. Stuart, J. A. K. Harmony and L. A. Kaplan. 1990. Development of a competitive enzyme-linked immunosorbent assay (ELISA) for a new apoprotein (J). *Clin. Chem.* **36**: 963.
15. de Silva, H. V., J. A. K. Harmony, W. D. Stuart, C. M. Gil, and J. Robbins. 1990. Apolipoprotein J: structure and tissue distribution. *Biochemistry.* **29**: 5380-5389.
16. Feinberg, A. P., and B. Vogelstein. 1983. A technique for radiolabeling DNA restriction endonuclease fragments to high specific activity. *Anal. Biochem.* **132**: 6-13.
17. Yanisch-Perron, C., J. Vieira, and J. Messing. 1985. Improved M13 phage cloning vectors and host strains: nucleotide sequences of the M13mp18 and pUC19 vectors. *Gene.* **33**: 103-119.
18. Duncan, C. H. 1985. Quasi-end labeling in M13 dideoxy sequence analysis. *NEN Product News.* **4**: 6-7.
19. Frohman, M. A., M. K. Dush, and G. R. Martin. 1988. Rapid production of full-length cDNAs from rare transcripts by amplification using a single gene-specific oligonucleotide primer. *Proc. Natl. Acad. Sci. USA.* **85**: 8998-9002.
20. Sanger, F., S. Nicklen, and A. R. Coulson. 1977. DNA sequencing with chain-terminating inhibitors. *Proc. Natl. Acad. Sci. USA.* **74**: 5463-5467.
21. Chomczynski, P., and N. Sacchi. 1987. Single-step method of RNA isolation by acid guanidinium thiocyanate-phenol-chloroform extraction. *Anal. Biochem.* **162**: 156-159.
22. Krakowsky, J. M., E. S. Panke, R. F. Lee, J. McNeish, S. S. Potter, and J. B. Lingrel. 1989. Analysis of possible repressor elements in the 5'-flanking region of the human  $\beta$ -globin gene. *DNA.* **8**: 715-721.
23. Nishina, P. M., J. Verstuyft, and B. Paigen. 1990. Synthetic low and high fat diets for the study of atherosclerosis in the mouse. *J. Lipid Res.* **31**: 859-869.
24. Witte, D. P., D. A. Wiginton, J. J. Hutton, and B. J. Aronow. 1991. Coordinate developmental regulation of purine catabolic enzyme expression in gastrointestinal and postimplantation reproductive tracts. *J. Cell Biol.* **115**: 179-190.
25. Fitzgerald, M., and T. Shenk. 1981. The sequence 5'-AAUAAA-3' forms part of the recognition site for polyadenylation of late SV40 mRNAs. *Cell.* **24**: 251-260.
26. Kozak, M. 1986. Point mutations define a sequence flanking the AUG initiator codon that modulates translation by eukaryotic ribosomes. *Cell.* **44**: 283-292.
27. Kirszbaum, L., J. A. Sharpe, B. Murphy, A. J. F. d'Apice, B. Classon, P. Hudson, and I. D. Walker. 1989. Molecular cloning and characterization of the novel, human complement-associated protein, SP40,40: a link between the complement and reproductive systems. *EMBO J.* **8**: 711-718.
28. Jenne, D. E., and J. Tschopp. 1989. Molecular structure and functional characterization of a human complement cytotoxicity inhibitor found in blood and seminal plasma: identity to sulfated glycoprotein 2, a constituent of rat testis fluid. *Proc. Natl. Acad. Sci. USA.* **86**: 7123-7127.
29. Collard, M. W., and M. D. Griswold. 1987. Biosynthesis and molecular cloning of sulfated glycoprotein 2 secreted by rat Sertoli cells. *Biochemistry.* **26**: 3297-3303.
30. Kelso, G. J., T. L. Kirley, and J. A. K. Harmony. 1991. Analysis of disulfide bonds within the novel apolipoprotein J isolated from human plasma. In *Techniques in Protein Chemistry II*. J. J. Villafranca, editor. Academic Press, New York. 305-312.
31. Kirszbaum, L., S. E. Bozas, and I. D. Walker. 1992. SP40,40, a protein involved in the control of the complement pathway, possesses a unique array of disulfide bridges. *FEBS Lett.* **297**: 70-76.
32. Kirszbaum, L., B. Murphy, and I. D. Walker. 1990. Molecular studies on SP40,40, a protein involved in both the complement pathway and the reproductive system. XIII Int. Complement Workshop. 354.
33. Wong, P., J. Pineault, J. Lakins, D. Taillefer, J. Léger, C. Wang, and M. Tenniswood. 1993. Genomic organization of the rat TRPM-2 (clusterin) gene, a gene implicated in apoptosis. *J. Biol. Chem.* **268**: 5021-5031.
34. Prakash, O., C. Kozak, and N. H. Sarkar. 1985. Molecular cloning, characterization, and genetic mapping of an endogenous murine mammary tumor virus proviral unit I of C3H/He mice. *J. Virol.* **54**: 285-294.
35. Taylor, B. A. 1978. Recombinant inbred strains—use in



- gene mapping. In *Origins of Inbred Mice*. H. C. Morse III, editor. Academic Press, New York. 423-438.
36. Elliott, R. W., L. C. Samuelson, M. S. Lambert, and M. H. Meisler. 1986. Assignment of pancreatic ribonuclease gene to mouse chromosome 14. *Cytogenet. Cell Genet.* **42**: 110-112.
37. Birkenmeier, E. H., V. A. Letts, W. N. Frankel, B. S. Magenheimer, and J. C. Calvet. 1993. Sulfated glycoprotein-2 (Sgp-2) maps to mouse chromosome 14. *Mammal. Genome.* **4**: 131-132.
38. Slawin, K., I. S. Sawczuk, C. A. Olsson, and R. Buttyan. 1990. Chromosomal assignment of the human homologue encoding SGP-2. *Biochem. Biophys. Res. Commun.* **172**: 160-164.
39. Aronow, B. J., S. D. Lund, T. L. Brown, J. A. K. Harmony, and D. P. Witte. 1993. Apolipoprotein J expression at fluid-tissue interfaces: potential role in barrier cytoprotection. *Proc. Natl. Acad. Sci. USA.* **90**: 725-729.
40. Jackson, R. L., S. J. Busch, and A. D. Cardin. 1991. Glycosaminoglycans: molecular properties, protein interactions, and role in physiological processes. *Physiol. Rev.* **71**: 481-539.
41. Li, W.-H., M. Tanimura, C.-C. Luo, S. Datta, and L. Chan. 1988. The apolipoprotein multigene family: biosynthesis, structure-function relationships, and evolution. *J. Lipid Res.* **29**: 245-271.
42. Kaiser, E. T., and F. J. Kézdy. 1983. Secondary structures of protein and peptides in amphiphilic environments (a review). *Proc. Natl. Acad. Sci. USA.* **80**: 1137-1143.
43. Hartmann, K., J. Rauch, J. Urban, K. Parczyk, P. Diel, C. Pilarsky, D. Appel, W. Haase, K. Mann, A. Weller, and C. Koch-Brandt. 1991. Molecular cloning of a glycoprotein complex secreted by kidney cells in vitro and in vivo: a link between the reproductive system and the complement cascade. *J. Biol. Chem.* **266**: 9924-9931.
44. Tsuruta, J. K., K. Wong, I. B. Fritz, and M. D. Griswold. 1990. Structural analysis of sulphated glycoprotein 2 from amino acid sequence. *Biochem. J.* **268**: 571-578.
45. Tall, A. R., and D. M. Small. 1980. Body cholesterol removal: role of plasma high density lipoproteins. *Adv. Lipid Res.* **17**: 1-51.
46. Miller, G. J., and N. E. Miller. 1975. Plasma high density lipoprotein cholesterol in ischemic heart disease. *Lancet.* **1**: 16-19.
47. Rosenfeld, S. I., C. H. Packman, and J. P. Leddy. 1983. Inhibition of the lytic action of cell-bound terminal complement components by human high density lipoproteins and apoproteins. *J. Clin. Invest.* **71**: 795-808.
48. Seifert, P. S., and M. D. Kazatchkine. 1988. The complement system in atherosclerosis. *Atherosclerosis.* **73**: 91-104.
49. Seifert, P. S., and G. K. Hansson. 1989. Complement receptors and regulatory proteins in human atherosclerotic lesions. *Arteriosclerosis.* **9**: 802-811.
50. Vlaicu, R., F. Niculescu, H. G. Rus, and A. Cristea. 1985. Immunohistochemical localization of the terminal C5b-9 complement complex in human aortic fibrous plaque. *Atherosclerosis.* **57**: 163-177.
51. Schäfer, H., D. Mathey, F. Hugo, and S. Bhakdi. 1986. Deposition of the terminal C5b-9 complement complex in infarcted areas of human myocardium. *J. Immunol.* **137**: 1945-1949.
52. Niculescu, F., H. G. Rus, and R. Vlaicu. 1987. Immunohistochemical localization of C5b-9, S-protein, C3d and apolipoprotein B in human arterial tissues with atherosclerosis. *Atherosclerosis.* **65**: 1-11.
53. Hamilton, K. K., R. Hattori, C. T. Esmon, and P. J. Sims. 1990. Complement proteins C5b-9 induce vesiculation of the endothelial cell membrane and expose catalytic surface for assembly of the prothrombinase enzyme complex. *J. Biol. Chem.* **265**: 3809-3814.
54. Bettuzzi, S., R. A. Hiipakka, P. Gilna, and S. Liao. 1989. Identification of an androgen-repressed mRNA in rat ventral prostate as coding for sulphated glycoprotein 2 by cDNA cloning and sequence analysis. *Biochem. J.* **257**: 293-296.
55. Sawczuk, I. S., G. Hoke, C. A. Olsson, J. Connor, and R. Buttyan. 1989. Gene expression in response to acute unilateral ureteral obstruction. *Kidney Int.* **35**: 1315-1319.
56. Buttyan, R., C. A. Olsson, J. Pintar, C. Chang, M. Bandyk, P. Y. Ng, and I. S. Sawczuk. 1989. Induction of the TRPM-2 gene in cells undergoing programmed death. *Mol. Cell. Biol.* **9**: 3473-3481.
57. Duguid, J. R., C. W. Bohmont, N. Liu, and W. W. Tourtellotte. 1989. Changes in brain gene expression shared by scrapie and Alzheimer disease. *Proc. Natl. Acad. Sci. USA.* **86**: 7260-7264.
58. May, P. C., M. Lampert-Etchells, S. A. Johnson, J. Poirier, J. N. Masters, and C. E. Finch. 1990. Dynamics of gene expression for a hippocampal glycoprotein elevated in Alzheimer's disease and in response to experimental lesions in rat. *Neuron.* **6**: 831-839.
59. Yokode, M., R. E. Hammer, S. Ishibashi, M. S. Brown, and J. L. Goldstein. 1990. Diet-induced hypercholesterolemia in mice: prevention by overexpression of LDL receptors. *Science.* **250**: 1273-1275.
60. Piedrahita, J. A., S. H. Zhang, J. R. Hagaman, P. M. Oliver, and N. Maeda. 1992. Generation of mice carrying a mutant apolipoprotein E gene inactivated by gene targeting in embryonic stem cells. *Proc. Natl. Acad. Sci. USA.* **89**: 4471-4475.
61. Zhang, S. H., R. L. Reddick, J. A. Piedrahita, and N. Maeda. 1992. Spontaneous hypercholesterolemia and arterial lesions in mice lacking apolipoprotein E. *Science.* **258**: 468-471.
62. Rubin, E. M., R. M. Krauss, E. A. Spangler, J. G. Verstuyft, and S. M. Clift. 1991. Inhibition of early atherogenesis in transgenic mice by human apolipoprotein A-I. *Nature.* **353**: 265.
63. Agellon, L. B., A. Walsh, T. Hayek, P. Moulin, X. C. Jiang, S. A. Shelanski, J. L. Breslow, and A. R. Tall. 1991. Reduced high density lipoprotein cholesterol in human cholesteryl ester transfer protein transgenic mice. *J. Biol. Chem.* **266**: 10796-10801.
64. Warden, C. H., C. C. Hedrick, J.-H. Qiao, L. W. Castellani, and A. J. Lusis. 1993. Atherosclerosis in transgenic mice overexpressing apolipoprotein A-II. *Science.* **261**: 469-472.